

Magnetotransport properties through phase transitions in $R_2\text{Fe}_{14}\text{B}$ ($R = \text{Y}, \text{Nd}, \text{Tm}$) compounds

Jolanta Stankiewicz* and Juan Bartolomé

*Instituto de Ciencia de Materiales de Aragón, Consejo Superior de Investigaciones Científicas,
and Universidad de Zaragoza, 50009-Zaragoza, Spain*

Satoshi Hirosawa

Sumitomo Special Metals Company Ltd., Egawa, Shimamotocho, Mishimagun, Osaka 618, Japan

(Received 25 October 2000; revised manuscript received 12 January 2001; published 14 August 2001)

The electrical resistivity and Hall effect of $\text{Y}_2\text{Fe}_{14}\text{B}$ single crystals have been measured over the temperature range of 4–700 K in magnetic fields of up to 5 T. From these and previous results, which we obtained for $\text{Nd}_2\text{Fe}_{14}\text{B}$ and $\text{Tm}_2\text{Fe}_{14}\text{B}$ single crystals, we draw some general conclusions about $R_2\text{Fe}_{14}\text{B}$ alloys. The overall behavior of the resistivity is determined mainly by Fe atoms; however, contributions from rare-earth atoms are clearly observed at low temperatures. Large variations of the Hall resistivity are found near the spin reorientation and Curie temperatures. They can be attributed to critical magnetization fluctuations which enhance skew scattering in these regions. We calculate spin fluctuations making use of a phenomenological molecular-field model for an anisotropic ferromagnet. Our calculations account quite well for the observed anomalies in the spontaneous Hall coefficient. Away from the critical regions, side-jump scattering of charge carriers seems to be responsible for the Hall effect.

DOI: 10.1103/PhysRevB.64.094428

PACS number(s): 75.50.Bb, 72.15.-v

I. INTRODUCTION

Transport properties of magnetic materials have been the subject of rather intensive research, both experimental and theoretical, for the last few decades. They can reveal interesting aspects, particularly when going through phase transitions. Recent developments in experimental techniques have made good-quality single-crystal materials available and enabled precise determination of transport properties. The interpretation of the experimental results thus obtained may sometimes be controversial, but they can also open up new areas of research.

It is well established that electron transport properties are very sensitive to electronic structure as well as to the magnetic nature of materials. Spectacular effects can be observed, especially when a magnetic field is applied. The conductivity of rare-earth metals shows anomalous behavior because the magnetism of the inner $4f$ shell strongly affects not only current carrier scattering but their band structure as well.¹ The effect of the s - f exchange interaction on the conductivity^{2,3} is also important in transport properties of intermetallic compounds with nontransition metals⁴ and of magnetic alloys.⁵ In particular, it may lead to anisotropy in magnetoresistance. Variations of the electrical resistivity with temperature and magnetic field provide relevant information about how itinerant magnetic electrons are.⁶ On the other hand, asymmetric current carrier scattering which is subject to spin-orbit interactions gives rise to a magnetization-dependent Hall effect.⁷ Its magnitude has been shown to be proportional to the third moment of the deviation of the magnetization from its mean value.^{8,9} Consequently, large variations of the anomalous Hall coefficient can be expected near critical points. These should be quite different through first-order transitions where spin fluctuations remain within bounds. It is our aim to study the resistivity and Hall effect in magnetic materials which show vari-

ous magnetic phase transitions in order to elucidate the role that different scattering mechanisms play in them and to pinpoint the interplay between electronic and magnetic phenomena. We choose to study intermetallic compounds of the type $R_2\text{Fe}_{14}\text{B}$ ($R = \text{Y}, \text{Nd},$ and Tm), which are important for technological applications as permanent magnets. The latter two show two different magnetic phase transitions while the former, which has a nonmagnetic R element, provides a reference for role that the $3d$ electrons play.

$R_2\text{Fe}_{14}\text{B}$ compounds crystallize in a tetragonal structure. Their magnetic properties are well known.^{10–12} In $R = \text{Nd}$ and Tm compounds there is competition between the strongly anisotropic magnetism of localized $4f$ electrons in rare-earth atoms and itinerant magnetism arising from $3d$ iron atoms. This gives rise to interesting physical properties.^{10–12} On the other hand, $\text{Y}_2\text{Fe}_{14}\text{B}$ has no $4f$ electrons. Its magnetic properties are completely determined by the Fe sublattice which shows uniaxial anisotropy along the tetragonal c axis. In $\text{Nd}_2\text{Fe}_{14}\text{B}$ and $\text{Tm}_2\text{Fe}_{14}\text{B}$, R and Fe sublattice moments couple ferromagnetically and antiferromagnetically, respectively. Upon cooling down from the Curie temperature, the magnetic structure of these compounds changes. In $\text{Tm}_2\text{Fe}_{14}\text{B}$, it occurs at approximately 311 K and consists of a discontinuous change of the net magnetization orientation from the c axis to the basal plane. In $\text{Nd}_2\text{Fe}_{14}\text{B}$, the net magnetization begins to tilt away (continuously) from the c axis, below approximately 135 K, to form a complex noncollinear ground state. Thus, two distinct types of spin-reorientation transition (SRT) are encountered in these materials. The ferromagnetic-paramagnetic transition is continuous; the Curie temperature T_c lies in the range (540–590) K for $R = \text{Y}, \text{Nd},$ and Tm . First-order magnetization process transitions have been observed in $\text{Nd}_2\text{Fe}_{14}\text{B}$ at high magnetic fields.¹³

In spite of the abundance of reports on the magnetic properties of $R_2\text{Fe}_{14}\text{B}$, only a few short ones have been devoted

to their electron transport properties. Resistivity anomalies at the SRT temperature have been found in $\text{Nd}_2\text{Fe}_{14}\text{B}$ and $\text{Tm}_2\text{Fe}_{14}\text{B}$.¹⁴ Anomalous electron transport in $\text{Nd}_2\text{Fe}_{14}\text{B}$ and $\text{Y}_2\text{Fe}_{14}\text{B}$ has been reported.¹⁵ Our own earlier papers have dealt with electron-transport properties of polycrystalline $R_2\text{Fe}_{14}\text{B}$ compounds¹⁶ and magnetotransport properties of $\text{Nd}_2\text{Fe}_{14}\text{B}$ and $\text{Tm}_2\text{Fe}_{14}\text{B}$ single crystals.^{17–19} From new results for $\text{Y}_2\text{Fe}_{14}\text{B}$ single crystals and other results we have previously obtained we draw some general conclusions.

In this paper we report the results of electrical resistivity and Hall effect measurements in $R_2\text{Fe}_{14}\text{B}$ ($R = \text{Y}, \text{Nd},$ and Tm) single crystals in a wide temperature range (4–700 K) and in magnetic fields of up to 5 T. The measurements were performed for various magnetic field orientations with respect to the easy-magnetization axis. The overall behavior of the resistivity is determined mainly by Fe atoms in these alloys. However, contributions from rare-earth atoms are observed clearly at low temperatures. Large variations of the Hall resistivity are encountered in the vicinity of both the spin-reorientation and paramagnetic-ferromagnetic transitions. The results obtained enable us to determine the dominant electron scattering processes and salient mechanisms underlying the Hall effect. A phenomenological molecular-field model for an anisotropic ferromagnet, which we use to calculate magnetization fluctuations, seems to account rather well for the observed features in the spontaneous Hall effect (SHE) coefficient in all the samples studied.

The experimental procedure is described in Sec. II. The results of resistivity and Hall effect measurements are reported and discussed in Sec. III. Conclusions are drawn in Sec. IV.

II. EXPERIMENT

We grew single crystals of $R_2\text{Fe}_{14}\text{B}$ using the floating-zone melting technique.²⁰ We measured the electrical resistivity and Hall effect on bar-shaped samples with a six-probe method. Samples were spark cut from a bulk single crystal. Their typical dimensions were $1 \times 1.5 \times 5 \text{ mm}^3$. We determined their crystallographic orientations by x-ray diffraction. Before measurements were made, each sample was polished and checked for possible cracks. Contact leads were ultrasonically soldered to the samples for low-temperature measurements. We used platinum pressure contacts in the high-temperature range. The specimens were mounted between two fixed copper plates on a sample holder to minimize thermal gradients and to avoid the effects of the large anisotropy torques on the samples when the external magnetic field was applied along the hard directions.

The Hall resistivity ρ_H was measured as a function of magnetic field up to 0.6 T at all experimental points. In addition, the variation of ρ_H with magnetic field, up to 5 T, was checked at 5, 100, and 280 K. These data and the magnetization measurements were made simultaneously with a superconducting quantum interference device (SQUID) magnetometer. For temperatures higher than 400 K the magnetization was measured with a Faraday balance.

We made use of two different configurations in our measurements. For $R = \text{Y}$ and Nd , the current flow was always

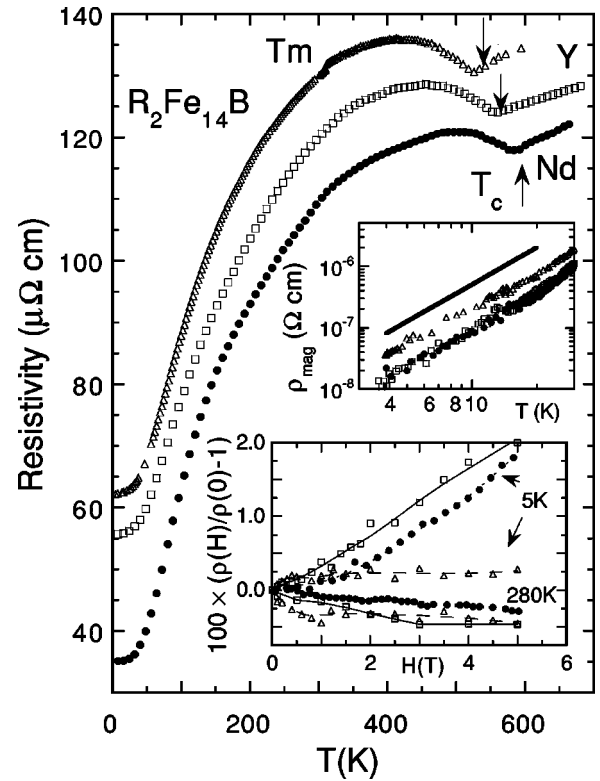


FIG. 1. Resistivity data points vs temperature in $R_2\text{Fe}_{14}\text{B}$ ($R = \text{Y}, \text{Nd},$ and Tm) single crystals. The upper inset exhibits the magnetic contribution to the resistivity vs T in the temperature range $4 \text{ K} \leq T \leq 30 \text{ K}$. The solid line shows a T^2 dependence. Variation of the electrical resistivity with the external magnetic field at $T = 5$ and 280 K for the same samples is shown in the lower inset.

perpendicular to the c axis while the external magnetic field was perpendicular or parallel to it. The edges of $\text{Tm}_2\text{Fe}_{14}\text{B}$ sample did not come out quite parallel to the principal crystallographic axes. All measurements were performed with the current flowing along the longest dimension of the sample which was at 80° with respect to the c axis and perpendicular to the external field. In one of the two configurations, the external magnetic field was at an angle of about 20° with the $[100]$ direction. In the second one, the magnetic field was rotated by 90° towards the $[010]$ direction.

III. RESULTS AND DISCUSSION

A. Electrical resistivity

How the resistivity ρ of $R_2\text{Fe}_{14}\text{B}$ single crystals varies with temperature in the range from 4 to 700 K is shown in Fig. 1. The overall behavior of the resistivity is alike in these compounds. It also resembles the resistivity of polycrystalline $R_2\text{Fe}_{14}\text{B}$ samples which has already been discussed in detail.¹⁶ For temperatures below approximately 40 K, $\rho \cong \rho_0 + AT^2$ where ρ_0 is the constant residual resistivity. This variation comes from electron-magnon scattering. As the temperature increases, ρ is observed to rise rapidly up to $T \approx 0.5T_c$. This rise is faster than the $T^{5/3}$ that is predicted by spin fluctuations theory.⁶ At higher temperatures, ρ increases more slowly and exhibits a small dip near the Curie point. In

this temperature range, electrons scatter mainly against disordered spins although the effect of magnetovolume coupling in Fe sublattices is clearly seen near T_c .¹⁵ Above T_c , all spins are disordered and the magnetic resistivity saturates. As electrons also scatter against phonons, ρ increases nearly linearly with temperature thereafter.

We next discuss the low-temperature magnetic resistivity and change of resistivity with magnetic field since new results have been obtained for them. To estimate the spin contribution ρ_{mag} to the resistivity, we write the total resistivity as $\rho = \rho_0 + \rho_{ph} + \rho_{mag}$, where ρ_{ph} is the resistivity arising from electron-phonon scattering. It can be calculated using the Bloch-Grüneisen formula, with a value of 420 K for the Debye temperature.¹¹ A plot of ρ_{mag} ($=AT^2$) versus T is shown in the upper inset of Fig. 1 for $T \leq 30$ K for the alloys studied. A least-squares fit yields values of A equal to 1.0×10^{-9} , 0.97×10^{-9} , and 1.7×10^{-9} $\Omega \text{ cm K}^{-2}$ for $R=Y$, Nd , and Tm , respectively. We note that the coefficients A are strongly enhanced with respect to the usual values of electron-magnon scattering in ferromagnetic metals.²¹ Such a strong enhancement of the electrical resistivity is expected for nearly ferromagnetic materials when electron correlations in itinerant d bands are taken into account.⁶

The values of A found for $R=Y$ and Nd are nearly the same. Only one low-lying acoustic magnon mode (Fe-Fe highly dispersive mode) is expected in $Y_2Fe_{14}B$. On the other hand, inelastic neutron scattering experiments done on $Nd_2Fe_{14}B$ alloys show additional magnon modes which involve spins of both rare-earth and iron ions.²² Our result and the fact that $Nd_2Fe_{14}B$ and $Y_2Fe_{14}B$ have nearly the same spin-wave stiffness constant indicate that the Fe-Fe mode starts at a lower energy than the acoustic R -Fe mode in $Nd_2Fe_{14}B$.²³ It may also be so for the Tm compound, although the value of the coefficient A for $Tm_2Fe_{14}B$ is 70% larger than that for $Y_2Fe_{14}B$. Obviously, the R -Fe magnon modes are also important in the scattering of electrons for the Tm compound. Using the relation $\rho_{mag} \propto T^2/(J^2S)$, where J and S are the strengths of the exchange interaction and the atomic spins involved in a magnon mode, respectively, we get $J_{TmFe} \cong 0.23J_{FeFe}$. This corresponds to an exchange field of approximately 220 T, in good agreement with theoretical predictions²⁴ and the results of numerical fittings.²⁵

The effect of the magnetic field on the transverse resistivity of $R_2Fe_{14}B$ compounds we have studied is illustrated in the lower inset of Fig. 1 for two temperatures: 5 and 280 K. At low temperatures, a positive magnetoresistance is found for all samples. It reaches a value of 2% for $R=Y$ and Nd at 5 T; its value is much smaller for the Tm compound. On the other hand, the resistivity decreases slightly when a magnetic field H is applied at room temperature. According to current theory, ρ decreases because spin fluctuations are suppressed by the external magnetic field.^{6,26} However, the low-temperature behavior of $\rho(H)$ can be explained neither by spin fluctuation theory nor by classical magnetoresistance mechanisms. We attribute most of the variation of the resistivity with magnetic field to magnetization-dependent scattering mechanisms. We estimate that side-jump scattering, which is important in our samples (see below), does not, however, contribute appreciably to magnetoresistance.²⁷

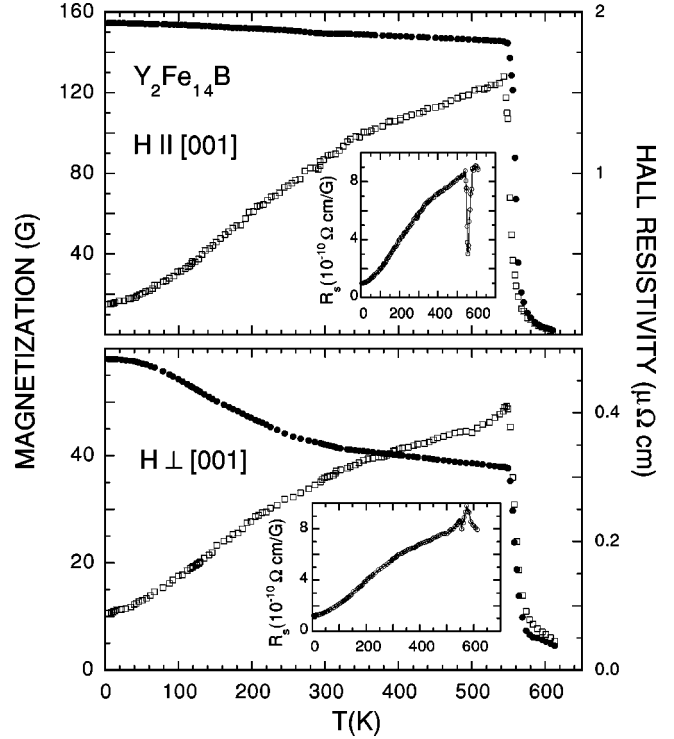


FIG. 2. Magnetization at $H=0.1$ T and the Hall resistivity as a function of temperature for $Y_2Fe_{14}B$ single crystal in two different magnetic-field directions. The insets show the anomalous Hall coefficient $R_s = \rho_H/4\pi M$ as a function of temperature.

Magnetic domain walls may also contribute to the resistivity.²⁸ We would expect their effect to saturate rapidly with magnetic field as the system becomes a single domain. Thus, we have presently no satisfactory explanation for the low-temperature magnetoresistance of $R_2Fe_{14}B$ alloys.

B. Hall effect

We now turn to a discussion of the Hall effect. The Hall resistivity ρ_H data are hole like and follow the magnetization of the sample up to 5 T at $T=5$, 100, and 280 K in all compounds we have examined. It implies that the Hall resistivity arises mainly from the anomalous Hall effect. The low-field Hall resistivity varies strongly with temperature. It is shown, in addition to the magnetization, in Fig. 2 for a $Y_2Fe_{14}B$ single crystal for two magnetic-field orientations with respect to the easy axis. ρ_H increases as T increases up to T_c , where it drops sharply to very low values. The same happens in other $R_2Fe_{14}B$ compounds we have studied. In addition, they show anomalous features near the SRT. Thus, for H perpendicular to the c axis, ρ_H passes through a sharp maximum near 130 K in $Nd_2Fe_{14}B$. For a parallel configuration, ρ_H shows no anomaly close to T_s and its variation with T is very similar to that of $Y_2Fe_{14}B$.¹⁸ In $Tm_2Fe_{14}B$, ρ_H exhibits a small maximum near T_s for both configurations studied.¹⁹

Phenomenologically, the Hall resistivity is given by $\rho_H = R_o B + R_s 4\pi M$, where R_o is the ordinary Hall coefficient, R_s is the SHE coefficient, B is the applied magnetic induc-

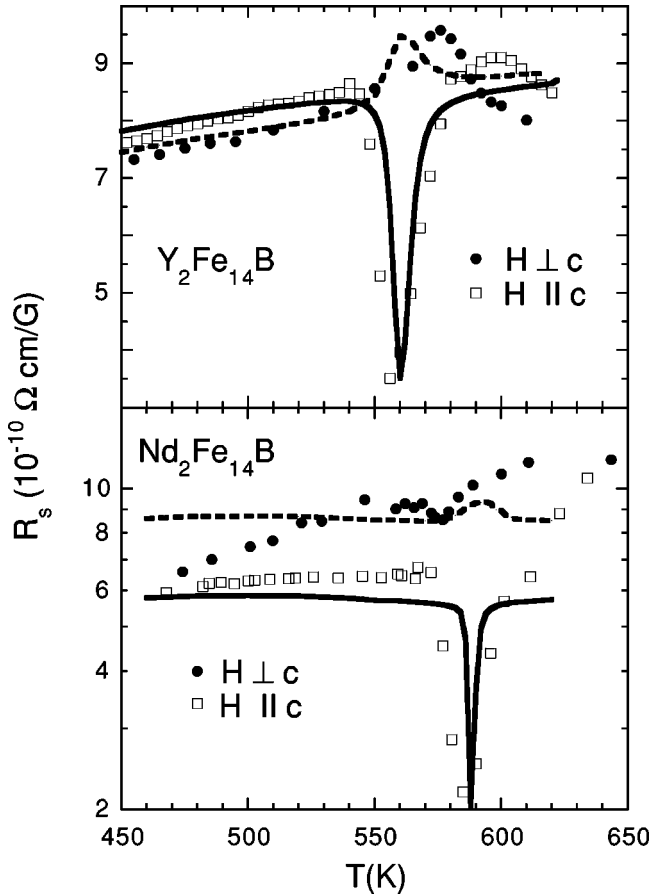


FIG. 3. High-temperature anomalous Hall coefficient for $Y_2Fe_{14}B$ and $Nd_2Fe_{14}B$ single crystals. The solid and dashed lines are fits to experimental points.

tion, and M is the spontaneous magnetization. In $R_2Fe_{14}B$, R_s is much larger than R_o ($R_o \leq 0.01R_s$).¹⁷ Therefore, we obtain values of the SHE coefficient from $R_s = \rho_H/4\pi M$. The anisotropy fields in $R_2Fe_{14}B$ compounds are high;¹² therefore the magnetic field we apply in our measurements (0.1 T) is too small to saturate the magnetization even in the easy direction. Consequently, we are in the linear part of the $M(B)$ and $\rho_H(B)$ curves, which depend on a particular shape of the sample. To avoid domain- and sample-shape-related effects, we measure M with the same field as ρ_H , applied to the same sample.

The temperature variations of R_s for $Y_2Fe_{14}B$ are shown in the inset of Fig. 2. For $\mathbf{H} \parallel [001]$, R_s shows a sharp minimum at T_c . On the other hand, for \mathbf{H} perpendicular to the c easy axis there is only a small rise in R_s at T_c . Such behavior through the Curie point has also been found for $Nd_2Fe_{14}B$ (see Fig. 3).¹⁸ It is alike in $Tm_2Fe_{14}B$; however, the crystallographic orientation of this sample does not allow a clear observation.¹⁹ In addition to the minimum at T_c , R_s shows extra features near the spin-reorientation transition. In $Nd_2Fe_{14}B$, a dip in R_s is encountered at T_s for $\mathbf{H} \perp [001]$; R_s drops slightly at T_s in $Tm_2Fe_{14}B$ in the configuration in which \mathbf{H} is nearly parallel to the $[100]$ axis (orientation 1). This is shown in Fig. 4. Away from the magnetic critical

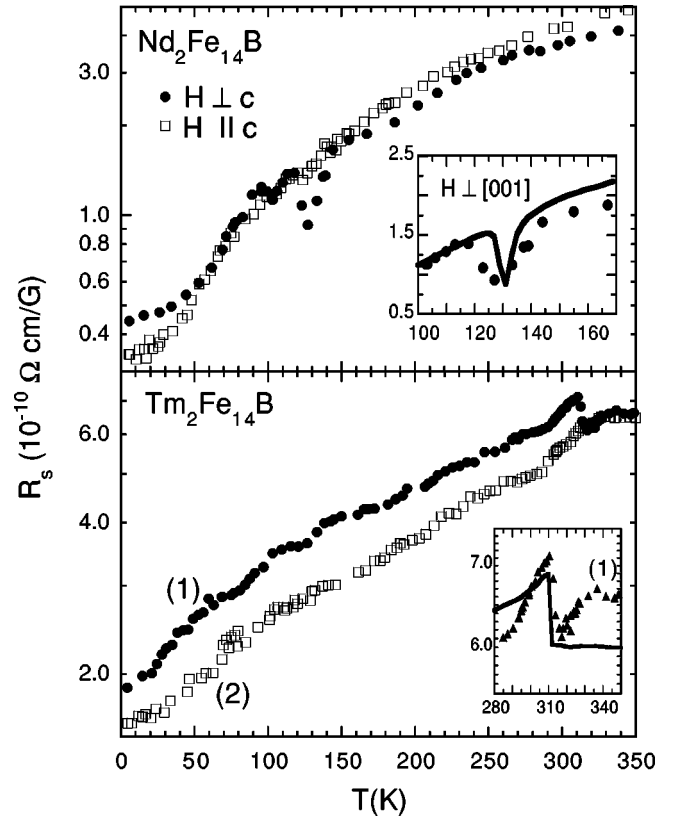


FIG. 4. Anomalous Hall coefficient as a function of temperature for $T \leq 350$ K in $Nd_2Fe_{14}B$ and $Tm_2Fe_{14}B$ single crystals. The orientation 1 (2) for $Tm_2Fe_{14}B$ corresponds to \mathbf{H} nearly parallel (perpendicular) to the $[100]$ low-temperature easy-axis direction. The insets show our fits (solid lines) to experimental points.

regions, $R_s \propto \rho^2$ for $R = Y$ and Nd . In the case of $R = Tm$, this relation is satisfied for $T \geq 170$ K and $T \leq 60$ K.

The behavior of the SHE coefficient in $R_2Fe_{14}B$ compounds can be explained in terms of skew and side-jump scattering mechanisms. In models with localized spins, the skew term gives $\rho_H \propto M_3$, where $M_3 = \langle (M_H - \langle M_H \rangle)^3 \rangle$, and M_H is the magnetization along the magnetic-field direction.^{8,9} Since magnetization fluctuations are large near the critical points, the observed variations of R_s near T_s and T_c likely come from them. The dependence of R_s on the orientation of the easy axis with respect to the magnetic field gives additional ground for this conclusion.¹⁸ On the other hand, in the vicinity of a first-order phase transition spin fluctuations are finite, except at the transition point. Consequently, no large variations of R_s are expected near such a point. This is how R_s behaves in $Tm_2Fe_{14}B$ (see Fig. 4).

In addition to skew scattering, a nonclassical effect of a side-jump Δy at scattering can be important in the SHE.²⁷ This mechanism, which also involves the spin-orbit interaction, gives $\rho_H \propto \rho^2 \langle M \rangle$. The variation of R_s with ρ for $R = Y$ and Nd is exhibited in Fig. 5. Here, the solid line shows a ρ^2 dependence. Indeed, we find that the experimental data follow this dependence quite closely. In the inset of Fig. 5, the R_s values at the lowest temperature measured are plotted against the values of residual resistivity in our samples. The solid line shows a fit to a relation $R_s = b\rho^2$ where b

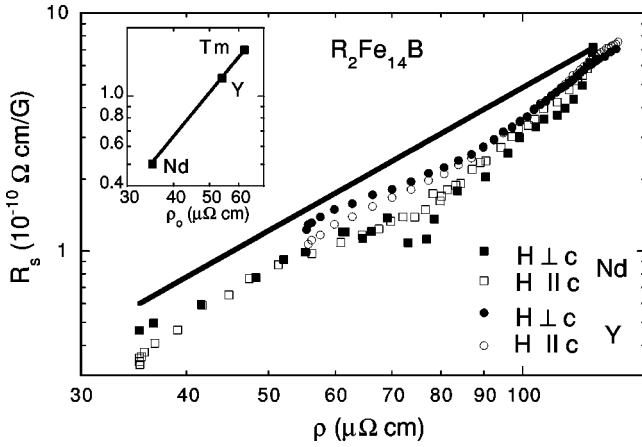


FIG. 5. Anomalous Hall coefficient R_s as a function of the total resistivity ρ for $Y_2Fe_{14}B$ and $Nd_2Fe_{14}B$ single crystals. The solid line shows a ρ^2 dependence. The inset exhibits a low-temperature R_s as a function of the residual resistivity for $R_2Fe_{14}B$ ($R=Y, Nd$, and Tm) single crystals.

$=0.04 \Omega^{-1} \text{cm}^{-1} \text{G}^{-1}$. Interestingly, this value is nearly equal to the values of b obtained from fittings discussed below. Consequently, we believe it is meaningful although the number of data points is very small. Therefore, away from critical points, ρ_H in $R_2Fe_{14}B$ seems to be limited by side-jump scattering as occurs in materials with large ρ .

Usually, a relation $R_s = a\rho + b\rho^2$ is satisfied between the SHE and the longitudinal resistivity.²⁹ Following results of Kondo⁸ and Maranzana,⁹ we fit the relation $R_s = aM_3/4\pi M + b\rho^2$, where the skew component is expressed in terms of spin fluctuations, to the experimental results. We have calculated the magnetization and its fluctuations within a phenomenological molecular-field model for an anisotropic ferromagnet^{30,25} which has been outlined in Ref. 17. In this model, the anisotropy energy (for tetragonal symmetry) is of the form $E_{an}^R = K_1 \sin^2 \theta + \tilde{K}_2 \sin^4 \theta + \tilde{K}_3 \sin^6 \theta$ and $E_{an}^{Fe} = K_0 \sin^2 \theta$ for the rare-earth and Fe ion, respectively.^{25,31} Here, K_1 , \tilde{K}_2 , \tilde{K}_3 , and K_0 are temperature-dependent uniaxial-anisotropy constants, and θ is the angle between the c axis and the magnetization vector. We assume that the R (\mathbf{m}_R) and Fe (\mathbf{m}_{Fe}) moments are collinear and that the R - R exchange is negligible.¹² The total magnetic energy of $R_2Fe_{14}B$ per unit cell can be written

$$E = 4E_{an}^R + 28E_{an}^{Fe} - (4\mathbf{m}_R + 28\mathbf{m}_{Fe}) \cdot \mathbf{H} - 56n_{RF}m_R m_{Fe} - 14n_{FF}m_{Fe} m_{Fe}, \quad (1)$$

where exchange-interaction coefficients (dimensionless) n_{RF} and n_{FF} describe the R -Fe and Fe-Fe magnetic interactions, respectively. We assume that $m_R(T)$ and $m_{Fe}(T)$ can be described by a Brillouin function with a corresponding molecular field for each component,¹²

$$m_R(T) = m_R(0) B_J[\mu_B \mathbf{m}_R(0) \cdot \mathbf{H}_R(T) / k_B T], \quad (2)$$

$$m_{Fe}(T) = m_{Fe}(0) B_{S_{Fe}}[\mu_B \mathbf{m}_{Fe}(0) \cdot \mathbf{H}_{Fe}(T) / k_B T], \quad (3)$$

where $\mu_R(0)$ and $\mu_{Fe}(0)$ are the zero-temperature moments of R and Fe, respectively, S_{Fe} is the Fe spin, J is the total angular momentum of the $4f$ electrons, k_B is the Boltzmann constant, and μ_B is the Bohr magneton. The molecular fields for the R and Fe moments are

$$\mathbf{H}_R(T) = \mathbf{H} + 14n_{RF} \mathbf{m}_{Fe}(T), \quad (4)$$

$$\mathbf{H}_{Fe}(T) = \mathbf{H} + [14n_{FF} \mathbf{m}_{Fe}(T) + 2n_{RF} \mathbf{m}_R(T)]. \quad (5)$$

For $Y_2Fe_{14}B$, $n_{RF} = 0$. Here $M(H, T)$ follows from the equilibrium condition $dE/d\theta = 0$. The spin-moment fluctuations have been obtained from the relation $\langle (M_H - \langle M_H \rangle)^3 \rangle = (k_B T)^2 (\partial^2 M_H / \partial H^2)_T$. Values of the anisotropy constant for $R=Y$ were taken from Ref. 20. We used the same anisotropy values as in Ref. 17 for $Nd_2Fe_{14}B$. For $Tm_2Fe_{14}B$, the corresponding values were taken from Ref. 13. However, we did not find how they change with temperature. We assumed a linear variation and that $K_{eff}(T) = K_0(T) + K_1(T) + \tilde{K}_2(T) + \tilde{K}_3(T) = 0$ at T_s . Values of 6×10^3 and of 1.1×10^4 for n_{FF} in $R=Nd$ and $R=Y$ and Tm compounds, respectively, and of 2×10^3 for n_{RF} give the best fit between the calculated and the measured magnetization at saturating field in $R_2Fe_{14}B$ alloys studied. The free-ion moment was used as the zero-temperature moment of Nd and Tm ions. We assume a value of $2.1 \mu_B$ for $\mu_{Fe}(0)$ and a value of 1 for the Fe spin.²⁰

Figure 3 exhibits the best fit (solid and dashed lines) to the spontaneous Hall coefficient in the high-temperature range for $Y_2Fe_{14}B$ and $Nd_2Fe_{14}B$ in the two configurations studied. Our calculations reproduce very well the observed pronounced negative peak at T_c for $\mathbf{H} \parallel [001]$ in both compounds. The low-temperature region is shown in Fig. 4 for $Nd_2Fe_{14}B$ and $Tm_2Fe_{14}B$. Here, the calculated R_s (solid lines) are exhibited in the insets for the perpendicular (or nearly perpendicular) orientation in Nd (Tm) alloy. Lack of knowledge of the anisotropy constants for the latter compound makes our calculations somewhat unreliable for it. Nevertheless, they reproduce correctly the behavior of R_s through the SRT as shown in the lower inset of Fig. 4. Our fits to R_s yield $b = 0.045(0.035) \Omega^{-1} \text{cm}^{-1} \text{G}^{-1}$ for both configurations and $a = 3.5 \times 10^{25}(1.6 \times 10^{24}) \Omega \text{cm}^{-5} \text{G}^{-3}$ in Y (Nd) compound for \mathbf{H} parallel to the c axis; $a = 1 \times 10^{25} \Omega \text{cm}^{-5} \text{G}^{-3}$ in $Nd_2Fe_{14}B$ for perpendicular orientation. These values are not far from the theoretically predicted ones.^{9,27} Berger has shown that $4\pi M_s b = ne^2 \Delta y / \hbar k$, where n and k are the electron concentration and wave vector, respectively.²⁷ Assuming $n = 3 \times 10^{22} \text{cm}^{-3}$, one obtains the length of the side-jump $\Delta y = 2 \times 10^{-9} \text{cm}$, which is quite close to the estimated one in ferromagnetic materials.²⁷ This is surprising, considering how rough our approximations are.

IV. CONCLUDING REMARKS

We have measured the resistivity and Hall effect of a $R_2Fe_{14}B$ ($R=Y, Nd$, and Tm) single crystals as a function of temperature and magnetic field. The overall behavior of these alloys is dominated by iron atoms although some interesting features follow from the presence of rare-earth atoms.

The low-temperature behavior of the magnetic resistivity ($\rho_{mag} \propto T^2$) arises quite likely from the scattering of electrons by magnons that involve iron atoms and both rare-earth and iron atoms. A strong enhancement of the electrical resistivity in this temperature region can be attributed to spin fluctuations in $R_2\text{Fe}_{14}\text{B}$ alloys which behave as nearly ferromagnetic materials. At high temperatures ($T > T_c$), the magnetic resistivity saturates but the total resistivity increases linearly with temperature owing to phonon scattering. The anomalous behavior of ρ just below T_c is most likely produced by strong lattice softening in this region.

The low-field Hall resistivity shows large variations near phase transition points. Such a behavior can be explained by magnetization fluctuations which enhance skew scattering in the critical regions of the spin reorientation and the paramagnetic-ferromagnetic transitions. Our results show

that the localized spin-charge carrier interaction is important therein. Following models in which the Hall resistivity and the third moment of the spin fluctuations are proportional, and calculating the latter within a molecular-field approximation for an anisotropic ferromagnet, we can reproduce quite well the observed anomalies in the SHE coefficient. Away from phase transition regions, the SHE seems to come from side-jump scattering, as it does in materials with large impurity concentrations. Magnetization-dependent scattering mechanisms also seem important for the magnetoresistance of $R_2\text{Fe}_{14}\text{B}$ alloys.

ACKNOWLEDGMENTS

This work was supported by Project MAT 99-1142 of Comisión Interministerial de Ciencia y Tecnología (CICYT).

*Electronic address: jolanta@posta.unizar.es

- ¹B. Coqblin, *The Electronic Structure of Rare-Earth Metals and Alloys: The Magnetic Heavy Rare-Earth* (Academic, London, 1977).
- ²T. Kasuya, *Prog. Theor. Phys.* **16**, 58 (1956).
- ³P.G. de Gennes and J. Friedel, *J. Phys. Chem. Solids* **4**, 71 (1958).
- ⁴E. Gratz and M.J. Zuckermann, in *Handbook on the Physics and Chemistry of Rare Earths*, edited by K. A. Gschneidner and L. Eyring (North-Holland, Amsterdam, 1982), Vol. 5, p. 117.
- ⁵A. Fert, *Physica B* **86-88**, 491 (1977).
- ⁶T. Moriya, in *Spin Fluctuations in Itinerant Electron Magnetism*, edited by M. Cardona, P. Fulde, and H.-J. Queisser, Springer Series in Solid-State Sciences Vol. 56 (Springer-Verlag, Berlin, 1985).
- ⁷C.M. Hurd, *Contemp. Phys.* **16**, 517 (1975).
- ⁸J. Kondo, *Prog. Theor. Phys.* **27**, 772 (1962).
- ⁹F.E. Maranzana, *Phys. Rev.* **160**, 421 (1967).
- ¹⁰K.H.J. Buschow, in *Ferromagnetic Materials, A Handbook on the Properties of Magnetically Ordered Substances*, edited by E. P. Wohlfarth and K.H.J. Buschow (North-Holland, Amsterdam, 1988), Vol. 4, p. 1.
- ¹¹E. Burzo and H.R. Kirchmayr, in *Handbook on the Physics and Chemistry of Rare Earths*, edited by K.A. Gschneidner and L. Eyring (Elsevier Science, Amsterdam, 1989), Vol. 12, p. 71.
- ¹²J.F. Herbst, *Rev. Mod. Phys.* **63**, 819 (1991).
- ¹³See J.J.M. Franse and R.J. Radwański, in *Rare-earth Iron Permanent Magnets, Monographs on the Physics and Chemistry of Materials*, edited by J.M.O. Coey (Clarendon Press, Oxford, 1996), Vol. 54, and references therein.
- ¹⁴F.J. Lazaro, J. Bartolomé, R. Navarro, C. Rillo, F. Lera, L.M. Garcia, J. Chaboy, C. Pique, R. Burriel, D. Fruchart, and S. Miraglia, *J. Magn. Magn. Mater.* **83**, 289 (1990).
- ¹⁵J.B. Sousa, M.M. Amado, R.P. Pinto, V.S. Amaral, and M.E.

- Braga, *J. Phys.: Condens. Matter* **2**, 7543 (1990); J.B. Sousa, M.M. Amado, R.P. Pinto, M.A. Salgueiro, M.E. Braga, and K.H.J. Buschow, *ibid.* **3**, 4119 (1991).
- ¹⁶J. Stankiewicz and J. Bartolomé, *Phys. Rev. B* **55**, 3058 (1997).
- ¹⁷J. Stankiewicz and J. Bartolomé, *Phys. Rev. B* **59**, 1152 (1999).
- ¹⁸J. Stankiewicz and J. Bartolomé, *Phys. Rev. Lett.* **83**, 2026 (1999).
- ¹⁹J. Stankiewicz, J. Bartolomé, and S. Hirosawa, *J. Phys.: Condens. Matter* **13**, 303 (2001).
- ²⁰S. Hirosawa, Y. Matsuura, H. Yamamoto, S. Fujimura, M. Saguawa, and H. Yamauchi, *J. Appl. Phys.* **59**, 873 (1986).
- ²¹I.A. Campbell and A. Fert, in *Ferromagnetic Materials, A Handbook on the Properties of Magnetically Ordered Substances*, edited by E.P. Wohlfarth (North-Holland, Amsterdam, 1982), Vol. 3, p. 763.
- ²²H.M. Mayer, M. Steiner, N. Stüßer, H. Weinfurter, B. Dorner, P.A. Lindgård, K.N. Clausen, S. Hock, and R. Verhoef, *J. Magn. Magn. Mater.* **104-107**, 1295 (1992).
- ²³M. Loewenhaupt and P. Fabi, *J. Alloys Compd.* **207-208**, 146 (1994).
- ²⁴M. Fähnle, K. Hummler, M. Liebs, and T. Beuerle, *Appl. Phys. A: Solids Surf.* **57**, 67 (1993).
- ²⁵M. Yamada, H. Kato, H. Yamamoto, and Y. Nakagawa, *Phys. Rev. B* **38**, 620 (1988).
- ²⁶M. Shiga, Y. Kusakabe, Y. Nakamura, K. Makita, and M. Sagawa, *Physica B* **161**, 206 (1989).
- ²⁷L. Berger, *Phys. Rev. B* **2**, 4559 (1970).
- ²⁸R.P. van Gorkom, A. Brataas, and G.E.W. Bauer, *Phys. Rev. Lett.* **83**, 4401 (1999).
- ²⁹J.M. Luttinger, *Phys. Rev.* **112**, 739 (1958).
- ³⁰J.M. Cadogan, J.P. Gavigan, D. Givord, and H.S. Li, *J. Phys. F: Met. Phys.* **18**, 779 (1988).
- ³¹F. Bolzoni, O. Moze, and L. Pareti, *J. Appl. Phys.* **62**, 615 (1987).